In-situ high pressure X-ray diffraction studies of orthoferrite $SmFeO_3$*

Li Na-Na(李娜娜), Li Yan(李 岩), Li Hui(李 会), Tang Rui-Lian(唐瑞莲), Zhao Yong-Sheng(赵永胜), Han Dan-Dan(韩丹丹), Ma Yan-Mei(马艳梅), Cui Qi-Liang(崔启良), Zhu Pin-Wen(朱品文)†, and Wang Xin(王 欣)‡

State Key Laboratory of Superhard Materials, Jilin University, Changchun 130012, *China*

(Received 31 October 2013; revised manuscript received 24 November 2013; published online 10 April 2014)

The high-pressure behaviors of $SmFeO_3$ are investigated by angle-dispersive synchrotron X-ray powder diffraction under a pressure of up to 40.3 GPa at room temperature. The crystal structure of $SmFeO_3$ remains stable at up to the highest pressure. The different pressure coefficients of the normalized axial compressibility are obtained to be $\beta_a = 0.60 \times 10^{-3}$ GPa^{-1}, $\beta_b = 0.79 \times 10^{-3}$ GPa^{-1}, $\beta_c = 1.28 \times 10^{-3}$ GPa^{-1}, and the bulk modulus (B_0) is determined to be 293(3) GPa by fitting the pressure–volume data using the Birch–Murnaghan equation of state. Furthermore, the larger compressibility of the FeO_6 octahedra suggests the evolution of the orthorhombic structure towards higher symmetry configuration at high pressures.

Keywords: crystal structure, high-pressure, X-ray diffraction

PACS: 91.60.Gf, 61.05.cp, 61.50.–f **DOI:** 10.1088/1674-1056/23/6/069101

1. Introduction

The rare-earth orthoferrites $RFeO_3$ (R = rare earth) that normally crystallize into a distorted orthorhombic structure with space group *Pnma* ($Z = 4$) are the derivative of an ideal cubic perovskite. From a structural point of view, the unit cell contains four equivalent Fe^{3+} ions situated at the octahedral center surrounded by six nearest-neighbor O atoms and the Fe–O–Fe superexchange angle is in a range of $157^\circ > \phi > 142^\circ$ (for R varying from La to Lu).[1,2] Owing to the unique physical and chemical properties, these compounds are promising for a variety of potential applications, such as catalysts, gas separators, cathodes of solid oxide fuel cells, sensor materials, magneto-optic materials, spin valves, etc.[3–12] $SmFeO_3$, as one of the rare-earth orthoferrites, has attracted much attention due to its remarkable physical properties, such as colossal dielectric constant of 10^4 at room temperature, the enhanced magnetic couplings, high T_N temperature (T_N = 674 K), and spontaneous magnetization reversal at cryogenic temperatures.[13–16]

It is known that an important mechanism responsible for the degradation and even complete collapse of the magnetic state at very high density is the electronic process of a high-spin (HS)-to-low-spin (LS) transition resulting from a breakdown of Hund's rule at extreme pressures.[17–19] The antiferromagnetic insulators $RFeO_3$ (R = Pr, Eu, Lu) have demonstrated themselves for such an HS–LS transition in Fe^{3+} under high pressures, under which the process was also accompanied by a reversible first-order isostructural phase transition.[20] The pressure-induced magnetic transition from an antiferromagnetic to a paramagnetic insulating state has been observed in $BiFeO_3$.[21] Moreover, electronic and magnetic transitions were also observed in $GaFeO_3$ under high pressure.[22] Recently, $LaFeO_3$ was revealed to show a transition from magnetic to nonmagnetic state (at room temperature) at 30 GPa.[23] The quenched nonmagnetic state was explained as the transition of the Fe^{3+} ions from the HS state $S = 5/2$ to the LS state $S = 1/2$ (spin crossover). In this paper, we study the *in-situ* structural properties of $SmFeO_3$ at high pressures. The results are conducive to a better understanding of the electrical and magnetic properties of $SmFeO_3$ under high pressure.

2. Experimental methods

Sm_2O_3 (99.99% purity), $Fe(NO_3)_3{\cdot}9H_2O$ (99.9% purity), and citric acid (AR) were used as raw materials. Sm_2O_3 was dissolved in nitric acid and diluted in distilled water. $Fe(NO_3)_3{\cdot}9H_2O$ was added to the distilled water and mixed with the Sm nitrates in stoichiometric ratio of Sm:Fe = 1:1. Citric acid was then added as a fuel to the above solution to yield a citrate/nitrate ratio of 1.2. The mixed solution was continuously stirred using a magnetic agitator. The solution was evaporated by heating at 353 K until a brown sticky gel was formed. Subsequently, the gel was dried at a temperature of up to 423 K. The dried gel was calcined at 1073 K in air for 10 h by intermediate grinding and pelletizations.

*Project supported by the National Natural Science Foundation of China (Grant No. 51172091), the Program for New Century Excellent Talents in University, China, and the National Fund for Fostering Talents of Basic Science, China (Grant No. J1103202).

†Corresponding author. E-mail: zhupw@jlu.edu.cn

‡Corresponding author. E-mail: xin_wang @jlu.edu.cn

© 2014 Chinese Physical Society and IOP Publishing Ltd

In the ambient condition, the phase purity was detected by powder X-ray diffraction (XRD) measurements using Rigaku Rotaflex X-ray diffractometer with Cu-K_α radiation at room temperature. *In-situ* high-pressure XRD experiments were carried out under up to 40.3 GPa using a synchrotron angle-dispersive X-ray source ($\lambda = 0.6199$ Å) of the 4W2 High-Pressure Station of Beijing Synchrotron Radiation Facility (BSRF). The diffraction data were collected using an MAR165 CCD detector. One of the as-prepared samples was loaded into a gasketed DAC with a 4:1 methanol/ethanol mixture as pressure-transmitting medium. Pressure was calibrated by the ruby luminescence method.[24]

3. Results and discussion

The crystal structure of as-prepared sample $SmFeO_3$ is consistent with the earlier report, and it has the orthorhombic symmetry (space group *Pnma*, $Z = 4$) at room temperature.[25] This orthorhombic structure of $SmFeO_3$ can be represented as a three-dimensional (3D) network of FeO_6 with Sm atoms occupying the interstitial spaces as shown in Fig. 1. The ambient-pressure diffraction pattern of $SmFeO_3$ was refined in the *Pnma* phase with lattice constants of $a = 5.5975(4)$ Å; $b = 7.7134(4)$ Å; $c = 5.4034(3)$ Å by the Rietveld method using GSAS software.[26] The refined pattern of $SmFeO_3$, together with the calculated peak profile and their differences and the merits of the refinement are presented in Fig. 2(a).

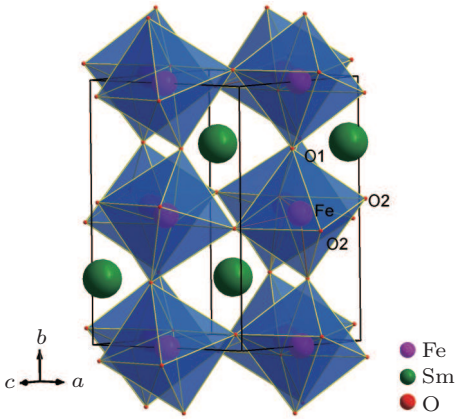


Fig. 1. (color online) Schematic representation of the crystal structure of $SmFeO_3$.

In order to study the structural behaviors of $SmFeO_3$ at high pressures, a synchrotron XRD experiment was performed. Powder diffraction patterns were collected at various pressures (up to 40.3 GPa). Figure 3 shows a few representative XRD patterns of $SmFeO_3$. It can be seen that all of the diffraction peaks shift towards higher 2θ values and exhibit some broadened features due to the non-hydrostatic conditions evolving with increasing pressure. No obvious changes can be found in the diffraction patterns, suggesting that the crystal structure of $SmFeO_3$ is stable up to the highest pressure. Rietveld refinements of the orthorhombic $SmFeO_3$ were carried out for all the pressures by using GSAS software. For example, figure 2(b) shows the refined pattern at 18.1 GPa with $R_p = 2.32\%$ and $R_{wp} = 3.13\%$.

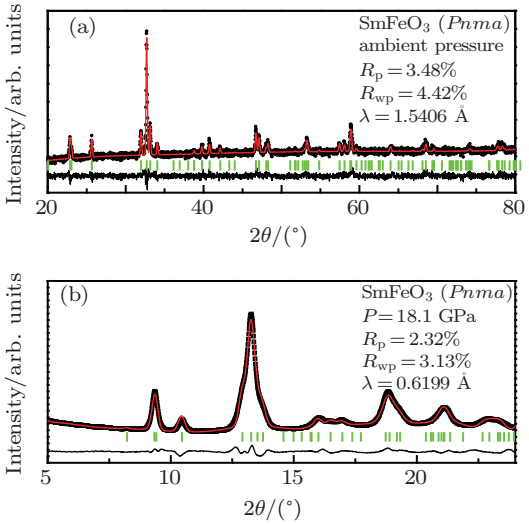


Fig. 2. (color online) Observed, calculated, and difference X-ray powder pattern of $SmFeO_3$ at ambient pressure (a) and 18.1 GPa (b).

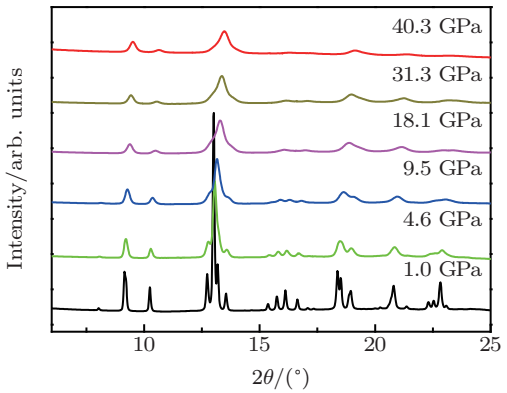


Fig. 3. (color online) Angle dispersive XRD patterns of $SmFeO_3$ at selected pressures with incident wavelength $\lambda = 0.6199$ Å at room temperature.

It has been reported that $RFeO_3$ (R = Eu, Lu, Pr) experienced a reversible first-order isostructural phase transition around 50 GPa, accompanied with an abrupt volume decrease (about 5%).[20] However, there is no abnormal change for $SmFeO_3$ up to 40.3 GPa. The pressure dependences of the lattice parameters of $SmFeO_3$ are shown in Fig. 4. As can be seen, the unit volume and lattice constants of $SmFeO_3$ decrease smoothly with increasing pressure, and no evidence of structural phase transitions can be observed throughout the pressure range. For the expected isostructural phase transformation of $SmFeO_3$, a much higher pressure may be needed. The pressure–volume data can be fitted by a third-order Birch–Murnaghan equation of state:

$$P = \frac{3.0}{2} B_0 \left[\left(\frac{V_0}{V} \right)^{7/3} - \left(\frac{V_0}{V} \right)^{5/3} \right]$$

$$\times \left\{1+\frac{3.0}{4}\left(B_0'-4\right)\times\left[\left(\frac{V_0}{V}\right)^{2/3}-1\right]\right\}, \quad (1)$$

where B_0 and B_0' are the bulk modulus and its pressure derivative at equilibrium volume V_0. By fitting the equation, B_0 is determined to be 293(3) GPa at a fixed $B_0' = 4$, and the value is comparable to the bulk modulus of some other ordered perovskites, such as $GaFeO_3$, $LuFeO_3$, and $EuFeO_3$ that have the bulk modulus of 296(25) GPa, 241(5) GPa, and 241(2.5) GPa respectively.[22,23,25] In $SmFeO_3$, the compression behaviors are different along its crystallographic axes. The different pressure coefficients of the normalized axial compressibility are obtained to be $\beta_a = 0.60\times10^{-3}$ GPa^{-1}, $\beta_b = 0.79\times10^{-3}$ GPa^{-1}, $\beta_c = 1.28\times10^{-3}$ GPa^{-1} with a linear fitting. Obviously, the compressibility in the c-axis direction is much larger than that in a–b plane. The anisotropic compressibility can in principle bring about some significant changes of its electronic properties, as observed in $NdFeO_3$ and $LuFeO_3$.[22,27]

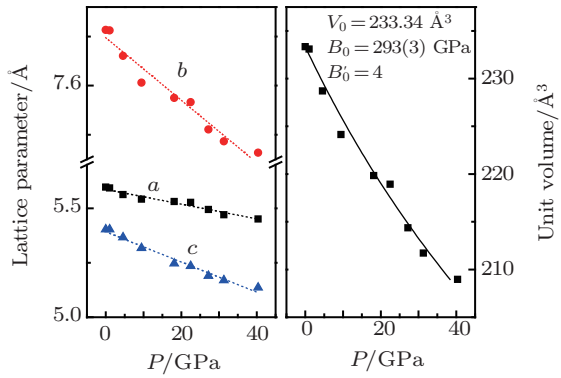


Fig. 4. (color online) Pressure dependences of the lattice constants and the unit cell volume of the orthorhombic $SmFeO_3$.

To further investigate the structural changes that will influence the magnetic property under high pressures, the pressure dependences of Fe–O bond length and Fe–O–Fe bond angle are presented in Fig. 5. The Jahn–Teller distortion of the FeO_6 octahedra produces three pairs of Fe–O bonds. One pair (Fe–O_1) is along the b axis and the other two pairs lie in the ac plane with one of Fe–O_2 bonds being long and the other being short, as shown in Fig. 1. The tilts of the FeO_6 octahedra yield Fe–O_2–Fe tilting angles in the ac plane and Fe–O_1–Fe tilting angles along the b direction. Compared with two Fe–O_2 bonds in the ac plane, the Fe–O_1 bond along the b axis is more susceptible to compression, as shown in Fig. 5(a). In addition, the Fe–O_1–Fe bond angle increases with increasing pressure while the Fe–O_2–Fe bond angle remains almost unchanged, as shown in Fig. 5(b). The variation of Fe–O–Fe bond angle at high pressures is consistent with the theoretical calculations of $SmFeO_3$ as the Fe–O_1–Fe bond angle is only slightly modified (less than 2.5°) below 12 GPa.[28] These results imply that the application of pressures leads to the decrease of the tilting of the two adjacent FeO_6 octahedra along the b axis. Moreover, they indicate that the distortion and tilts of the octahedra FeO_6 are suppressed under high pressures. It is known that the magnetic properties of $SmFeO_3$ are determined by the superexchange of Fe–O–Fe interactions, which leads to antiferromagnetic ordering with the Néel temperature $T_N = 674$ K.[14] With increasing pressure, the shortening of the interionic Fe–O distance and the enlarging of the Fe–O–Fe bond angle will increase the superexchange of Fe–O–Fe interactions and then enhance the magnetic property of $SmFeO_3$.[29] Zhao *et al.*[28] indicated that the magnitude of the weak magnetization of Fe^{3+} increased with increasing pressure. Also, for $RFeO_3$ (R = Nd, Lu), the relevant experiments confirmed the increase of T_N under high pressure.[29] Therefore, the enhanced magnetic interactions are expected in $SmFeO_3$, and the study of pressure effects on its magnetic and electrical properties will be undertaken in future work.

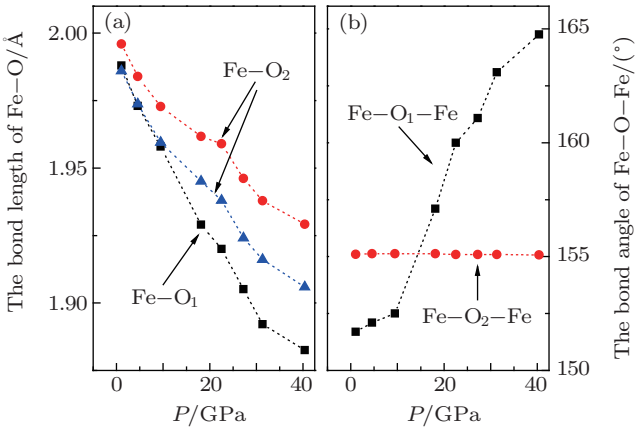


Fig. 5. (color online) Dependences of (a) bond length of Fe–O and (b) bond angle of Fe–O–Fe on pressure for the orthorhombic $SmFeO_3$.

Zhao *et al.*[28] used the bond-valence concept to develop their model, and indicated that in $GdFeO_3$-type orthorhombic perovskites (ABO_3) with both cations having a formal charge of 3+, the octahedral distortion and tilting should decrease with increasing pressure and the structure evolves towards a higher symmetry configuration with rising pressure, which is consistent with the recent single-crystal experimental results.[30,31] In general, the perovskite structure will become more distorted with increasing pressure if the BO_6 octahedra are less compressible than the RO_{12} polyhedra, or the structure will become less distorted at high pressures if the BO_6 octahedra are more compressible than the RO_{12} polyhedra.[32,33] As shown in Fig. 6, the volume change of the FeO_6 octahedron is more compressible than that of the unit cell. The V/V_0 of the FeO_6 octahedron is dependent on the Fe–O bond length and the O–Fe–O bond angle. The larger compressibility of the FeO_6 octahedron suggests the evolution of the orthorhombic structure towards higher symmetry configuration at high pressures. Our results are in good agreement with the results of

other studied orthorhombic perovskites, such as RMnO$_3$ (R = La, Tb, Gd).[34–36]

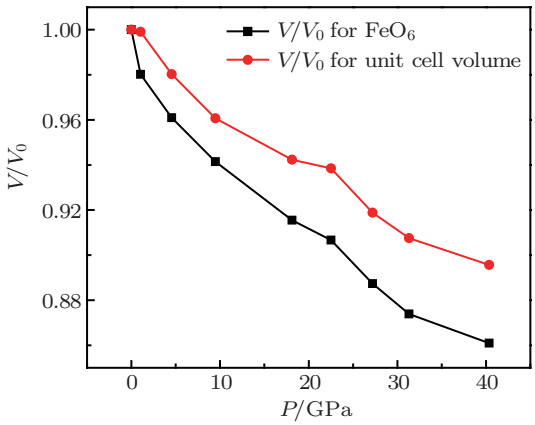


Fig. 6. (color online) Pressure dependences of the normalized volume of the FeO_6 octahedron and the unit cell.

4. Conclusions

In this paper, the high-pressure behaviors of orthoferrite $SmFeO_3$ are investigated by using angle-dispersive synchrotron X-ray powder diffraction at room temperature. The results indicate that the crystal structure is stable at a pressure of up to 40.3 GPa. From the refined diffraction patterns, the different axial compression coefficients of $SmFeO_3$ are obtained to be $\beta_a = 0.60 \times 10^{-3}$ GPa^{-1}, $\beta_b = 0.79 \times 10^{-3}$ GPa^{-1}, and $\beta_c = 1.28 \times 10^{-3}$ GPa^{-1}. This indicates that c axis is more compressible than a and b axes. The bulk modulus (B_0) is determined to be 293(3) GPa by fitting the pressure–volume data to the Birch–Murnaghan equation of state. In addition, the larger compressibility of the FeO_6 octahedron suggests the evolution of the orthorhombic structure towards higher symmetry configuration. Furthermore, the shortening of the interionic Fe–O distance and the lengthening of the Fe–O–Fe will enhance the magnetic property of $SmFeO_3$ with increasing pressure. Further work will focus on the pressure effect on the electronic structure in $SmFeO_3$.

Acknowledgment

The authors thank Dr. Li Yan-Chun for technical support with the high-pressure experiments at the 4W2 beamline of the BSRF synchrotron.

References

[1] Geller S and Wood E A 1956 *Acta Crystallogr.* **9** 563
[2] Lyubutin I S, Dmitrieva T V and Stepin A S 1999 *Zh. Éksp. Teor. Fiz.* **115** 1070
[3] Shen S T and Weng H S 1998 *Ind. Eng. Chem. Res.* **37** 2654
[4] Kharton V V, Yaremchenko A A, Kovalevsky A V, Viskup A P, Naumovich E N and Kerko P F 1999 *J. Membr. Sci.* **163** 307
[5] Kharton V V, Yaremchenko A A and Kharton E N 1999 *J. Solid State Electrochem.* **3** 303
[6] Kuscer D, Hrovat M, Hoic J, Bernik S and Kolar D 1996 *J. Power Sources* **61** 161
[7] Traversa E, Matsushima S, Okadab G, Sadaokab Y, Sakaib Y and Watanabe K 1995 *Sens. Actuators B* **25** 661
[8] Schmool D S, Keller N, Guyot M, Krishnan R and Tessier M 1999 *J. Appl. Phys.* **86** 5712
[9] Sakakima H, Satomi M, Hirota E and Adachi H 1999 *IEEE Trans. Magn.* **35** 2958
[10] Zheng L and Wu X S 2013 *Chin. Phys. B* **22** 107806
[11] Yang Y, Liu Y L, Zhu K, Zhang L Y, Ma S Y, Liu J and Jiang Y J 2010 *Chin. Phys. B* **19** 037802
[12] Wang H C, Wang C L, Zhang J L, Zhao M L, Liu J, Su W B, Yin N and Mei L M 2009 *Chin. Phys. Lett.* **26** 107301
[13] Prasad B V, Narsinga Rao G, Chen J W and Suresh Babu D 2011 *Mater. Res. Bull.* **46** 1670
[14] Kahn F J, Pershan P S and Remeika J P 1969 *Phys. Rev.* **186** 891
[15] Lee J H, Jeong Y K, Park J H, Oak M A, Jang H M, Son J Y and Scott J F 2011 *Phys. Rev. Lett.* **107** 117201
[16] Marshall L G, Cheng J G, Zhou J S, Goodenough J B, Yan J Q and Mandrus D G 2012 *Phys. Rev. B* **86** 064417
[17] Pasternak M P, Taylor R D, Jeanloz R, Li X, Nguyen J H and McCammon C A 1997 *Phys. Rev. Lett.* **79** 5046
[18] Li F Y, Jin C Q, Chen L C, Zhou B, Shi L C, Liu J, Li X D, Li Y C and Yu R C 2006 *Chin. Phys. Lett.* **23** 911
[19] Ge B H, Li F H, Li X M, Wang Y M, Chi Z H and Jin C Q 2008 *Chin. Phys. B* **17** 3163
[20] Rozenberg G Kh, Pasternak M P, Xu W M, Dubrovinsky L S, Carlson S and Taylor R D 2005 *Europhys. Lett.* **71** 228
[21] Gavriliuk A G, Struzhkin V V, Lyubutin I S, Hu M Y and Mao H K 2005 *JETP Lett.* **82** 224
[22] Arielly R, Xu W M, Greenberg E, Rozenberg G Kh, Pasternakl M P, Garbarino G, Clark S and Jeanloz R 2011 *Phys. Rev. B* **84** 094109
[23] Hearne G R, Pasternak M P, Taylor R D and Lacorre P 1995 *Phys. Rev. B* **51** 11495
[24] Mao H K and Bell P M 1978 *Carnegie Institution of Washington Year Book,* Vol. 77 (Washington: Carnegie Institute) p. 904
[25] Berenor A, Angoles E, Rossiny J, Raj E, Kilner J and Atkinson A 2008 *Solid State Ionics* **179** 1090
[26] Larson A C and Von Dreele R B 2004 *General Structure Analysis System (GSAS)*, Los Alamos National Laboratory Report LAUR **86** 748
[27] Aroyo M I, Perez-Mato J M, Capillas C, Kroumova E, Ivantchev S, Kirov A, Madariaga G and Wondratschek H 2006 *Z. Kristallogr.* **221** 15
[28] Zhao H J, Ren W, Yang Y R, Chen X M and Bellaiche L 2013 *J. Phys.: Condens. Matter* **25** 466002
[29] Gavriliuk A G, Stepanov G N, Lyubutin I S, Stepinb A S, Trojan I A and Sidorov V A 2000 *Hyperfine Interact.* **126** 305
[30] Angel R J, Zhao J, Ross N L, Jakeways C V, Redfern S A T and Berkowski M 2007 *J. Solid State Chem.* **180** 3408
[31] Ross N L, Zhao J and Angel R J 2004 *J. Solid State Chem.* **177** 3768
[32] Zhao J, Ross N L and Angel R J 2004 *Acta Crystallogr. B* **60** 263
[33] Zhao J, Ross N L and Angel R J 2004 *Acta Crystallogr. B* **60** 263
[34] Loa I, Adler P, Grzechnik A, Syassen K, Schwarz U, Hanfland M, Rozenberg G Kh, Gorodetsky P and Pasternak M P 2001 *Phys. Rev. Lett.* **87** 125501
[35] Chen J M, Chou T L, Lee J M, Chan T S, Lu K T, Chuang W T, Sheu H S, Chen S W, Lin C M, Hiraoka N, Tsuei K D and Yang T J 2009 *Phys. Rev. B* **79** 165110
[36] Lin C L, Zhang Y F, Liu J, Li X D, Li Y C, Tang L Y and Xiong L 2012 *J. Phys.: Condens. Matter* **24** 115402